

Regular and Reversible Rotation-Type Gas-Lubricated Conical Grooved Bearing

Shuzo SHIMADA*, Nobuyoshi KAWABATA**, Motoyoshi TACHIBANA** and Yasumi OZAWA***

(Received August 24, 2001)

A regular and reversible rotation type gas-lubricated conical grooved bearing is developed in this paper. Bearing characteristics of this new type of conical bearing are analyzed by the narrow groove theory. As a result, it is clarified that the present new type conical bearing generates the axial and radial characteristics at both regular and reverse rotations and bearing characteristics are almost a half of conventional one directional type conical grooved bearings. The bearing parameters which maximize each bearing characteristic (the axial load capacity, the radial load capacity and the mass of the stability limit) are decided. The bearing parameters, which improve both radial and axial characteristics in both directions of rotation, were decided.

Key Words: Machine Element, Gas Lubrication, Hydro-dynamic Bearing, Grooved Bearing, Conical Bearing, Regular and Reversible Rotation

1. Introduction

Gas-lubricated grooved bearings are available in various types including thrust circular-disk type, journal herringbone type, conical type and spherical type, among which the gas-lubricated conical grooved bearing features capability to receive both an axial load and a radial load at the same time. It has high reliability and the potential to reduce costs because it can be miniaturized. A study on the gas-lubricated conical grooved bearing was commenced by Muijderman^[1] and several other studies were reported later, some examples of which can be referred to in studies by Bootsma^[2], and Fukuyama/Someya^[3]. However, such conventional studies were made only for the case of one rotation direction.

The authors proposed a new idea which enables regular and reversible rotations for such gas-lubricated conical grooved bearings, and made studies on radial

characteristics of journal type bearings^[4] and axial characteristics of thrust circular-disk type bearings^[5]. As a result of such studies, we reported that the gas-lubricated conical grooved bearing offers satisfactory functions as a bearing, though the axial and radial load capacity will decrease by 50% when compared to those of conventional grooved bearings with one rotation direction. The present study refers to our considerations on bearing parameters which optimize the radial bearing characteristics when a system enabling regular and reversible rotations is applied on a conical bearing which receives both axial loads and radial loads at the same time.

The following shows important symbols and terms used thereafter:

c : bearing clearance (reference clearance)

ϕ : conical angle

D : reference diameter: For details, see Chapter 2.

A_0 : reference area, $\pi D^2/4$

A : total bearing area

A_1 : For regular and reversible rotation type, the

bearing area for the smooth part with larger radius (left part in Fig. 1)

For one directional rotation type, the bearing area for the grooved part with larger radius (left part in Fig. 2)

* Mechanical Engineering Course, Graduate School of Engineering

** Dept. of Mechanical Engineering

*** Dept. of Mechanical Engineering, Fukui Institute of Technology

A_2 : For regular and reversible rotation type, the bearing area for the grooved part with larger radius (the left part in Fig. 1)

For one directional rotation type, the bearing area for the smooth part.

A_3 : For regular and reversible rotation type, the bearing area for the grooved part with smaller radius (right part in Fig. 1).

For one directional rotation type, the bearing area for the grooved part with smaller radius (right part in Fig. 2).

A_4 : For regular and reversible rotation type, the bearing area for the smooth part with smaller radius (right part in Fig. 1)

δ, Δ : groove depth, $\Delta = \delta/c$

f_z, F_z : axial load capacity, $F_z = f_z(p_a \cdot D)/\sin \phi$

f_r, F_r : ingredient in radial direction of radial load capacity, $F_r = f_r(p_a \cdot D)/\cos^2 \phi$

m, M : mass of the stable limit,

$$M = m(p_a/D)(c/D)/\mu \cdot \cos^2 \phi$$

A : bearing number, $A = 6\mu \omega D^2/(c \cdot p_a)$

p_a : outside air pressure

μ : viscosity coefficient

ω : rotational angular velocity of bearing

α : groove width ratio

β : groove angle

γ_r : For regular and reversible rotation type,

$$\gamma_r = (A_1 + A_2)/A$$

γ_c : For one directional rotation type,

$$\gamma_c = A_1/(A_1 + A_3)$$

η : bearing area of smooth part area/total bearing area

For regular and reversible rotation type,

$$\eta = (A_1 + A_4)/A$$

For one directional rotation type, $\eta = A_2/A$

GMR : grooved member rotation

SMR : smooth member rotation

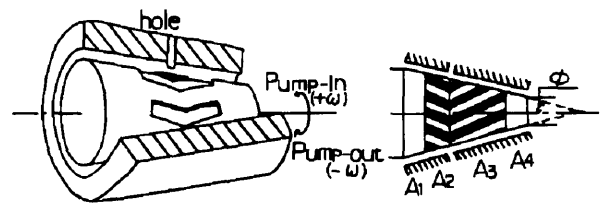
2. Regular and Reversible Rotation-Type Conical Bearing in the Present System

2.1 Structure and Operating Principle

Fig. 1 shows the regular and reversible rotation-type gas-lubricated conical grooved bearing as proposed in the present study. The bearing is provided with a herringbone groove, and it enables regular and reverse rotations by arranging a path hole leading to the outside air at the apex of the herringbone groove and by mounting a valve which opens only when outside air

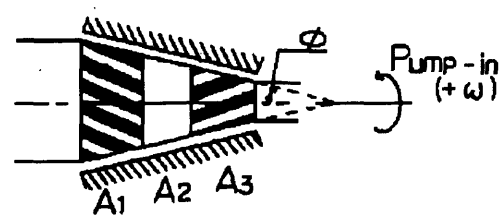
flows into the path hole. More specifically, the valve closes if the rotation is regular ($+\omega$), and the bearing functions as a pump-in type bearing, in which the lubricating air is thrust toward the bearing center due to the pumping effect caused by the groove, thus generating a positive pressure, and the valve opens if the rotation is reversed ($-\omega$), and the bearing functions as a pump-out type bearing which generates positive pressures, in which the operating gas is sucked into the bearing clearance via the path hole, thus generating a flow rate leading to the shaft end. For reference, a conventional one directional type gas-lubricated conical grooved herringbone bearing is illustrated in Fig. 2. Figures 1 and 2 respectively illustrate a bearing for the case of a grooved member rotation (hereinafter referred to as GMR) in which the grooved side rotates, but the case of a smooth member rotation (hereinafter referred to as SMR) in which the smooth side rotates is also referred to in this paper.

The area of respective regions on the shaft surface shall be defined as: A_1 for the smooth part at the left side (with larger radius); A_2 for the grooved part at the side to the left of the path hole; and A_3 and A_4 follows in the same way, as shown in Fig. 1. In this paper, the restriction $A_1/A_2 = A_4/A_3$ is given. For the bearing of one directional type, the area of the grooved parts at the left and the right sides shall be A_1 and A_3 respectively, and the area of the smooth part shall be A_2 as shown in Fig. 2. As parameters to specify profiles, β , α , Δ , γ_r , γ_c , and η shall be used.



$$\gamma_r = (A_1 + A_2)/A, \quad \eta = (A_1 + A_4)/A, \quad A_1/A_2 = A_4/A_3$$

Fig.1 Regular and reversible conical grooved bearing



$$\gamma_c = A_1/(A_1 + A_3), \quad \eta = A_2/A$$

Fig.2 Conventional conical grooved bearing

α , β , and Δ shall be of the same value in the region of A_2 and A_3 . In addition, γ_r shall be used for the regular and reversible rotation type as illustrated in Fig. 1 and indicates the ratio $(A_1 + A_2)/A$ of the shaft area for the part to the left of the path hole, while the total shaft area A and γ_c shall be used for the one directional rotation type as shown in Fig. 2, and be indicates ratio $(A_1/(A_1 + A_3))$ of the area of grooved part at the left aide and the area of total grooved parts. The parameter $\eta = (A_1 + A_4)/A$ is the ratio of the area of smooth part and the total bearing area A used for the regular and reversible rotation type illustrated in Fig. 1, while $\eta = A_2/A$ is used for the one directional rotation type illustrated in Fig. 2.

To determine the reference diameter D of a bearing, a cross-sectional diameter $D = \sqrt{(D_1^2 + D_2^2)/2}$ taken at a position that equally divides the bearing area was employed, considering the effect of conical angle ϕ . D_1 and D_2 are the maximum and minimum diameter of the conical bearing respectively.

For the bearing characteristics, further studies will be presented in the following section on the axial load capacity F_z , the ingredient in the eccentricity direction F_r of the radial load capacity and on the mass of the stable limit M . The Narrow Groove Theory [6], in which an infinite number of grooves is assumed, will be used for the analysis, and numeric calculations will be performed by using the method as described in Reference [7], and for the handling of the path hole, a similar handling method as described in Reference [4] will be used.

2.2 Effect of Conical Angle ϕ on Bearing Characteristics

In this study, the bearing characteristics f_z , f_r and m will be considered, but the conical angle ϕ of the

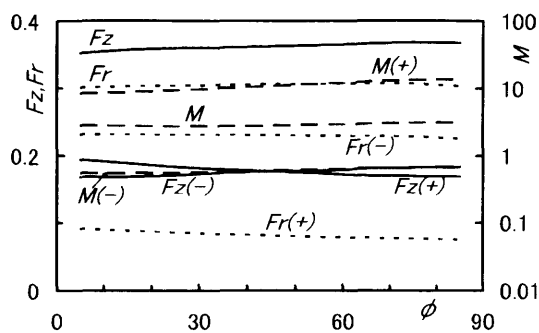


Fig3 Influences of ϕ for each characteristic (F_z, F_r, M)

bearing must be taken into account. Therefore, in producing dimensionless quantities, f_z was divided by $\sin \phi$, and f_r and m were divided by $\cos^2 \phi$ so that the effect of ϕ is minimized. Fig. 3 shows the effect of the conical angle ϕ of a bearing on these dimensionless bearing characteristics F_z , F_r , and M . It should be noted that the parameters used for the bearing are optimal parameters (referred to later in Table 1) which maximize F_z . The F_z shown in the figure stands for the conventional one directional rotation type, while $F_z(+)$ and $F_z(-)$ respectively are F_z at the time of regular rotation and reverse rotation of the regular and reversible-rotation type referred to in the present study. The same applies for F_r and M . The figure, shows the known result that various characteristics are hardly influenced by ϕ . In addition, Fig. 3 shows the result for GMR, and we have verified that, also in the case of SMR, all bearing characteristics are hardly influenced by ϕ and remain almost constant. The above, demonstrates that the chosen dimensionless quantities enables examinations over a wide range of conical angles without limiting us specific conical angles. In the following, considerations $\phi = 45^\circ$ will be assumed.

2.3 Stability Limit Mass M

Fig. 4 shows the relationship between the bearing number Λ and the mass M of the stable limit for the case of the regular rotation of GMR and SMR. It should be noted that, for the bearing parameters, the values in Table 3 (optimized parameters for M) described in Chapter 3 are used. For the case of SMR, M monotonously decreases as Λ increases. On the other hand, for the case of GMR, M monotonously decreases in the range where Λ is low, but it shows changes to a minimal value (point B), infinite (point E) and decreases sharply (points E \rightarrow C \rightarrow D). This is to be attributed to changes in the number of angular vibrations ν of the self-acting whirl. More specifically, this is because the mass of the stable limit is equivalent to the mass for which the centrifugal force (proportional to the mass m , the eccentricity degree and ν) and the ingredient in the eccentricity direction of reaction force in the lubrication film are balanced. And their reason is that mass is significantly influenced by ν/ω . Fig. 4 also illustrates the relationship between ν/ω and Λ . Normally in the low Λ region (of non-compressed nature), ν/ω becomes constant for both GMR and SMR (0.5 for bearing without grooves), and M will show

a flat decrease since the centrifugal force increases as Δ increases (corresponding to the increase of ω). In the case of SMR, a further increase of Δ will eventually increase the whirl angular velocity which results in the increase of the centrifugal force, thus decreasing the mass of the stable limit. Furthermore, in the case of GMR, ν/ω decreases as Δ increases, which will cause a decrease in the centrifugal force, thus increasing the mass of the stable limit. Accordingly, M will take the minimum value and become infinite as ν is nearing zero (0). When Δ gets larger, ν becomes negative, that is, the rotational direction of the whirl movement reverses, and the centrifugal force is generated again, whereby M will take finite values and decrease as Δ increases.

Accordingly, when for example an evaluation is made of the mass of the stable limit for $\Delta = 10$, it is necessary to make an evaluation while defining the minimum value of the mass of the stable limit in the region of 10 or less to be the mass of the stable limit of $\Delta = 10$, since Δ always go through the status of 10 or less before Δ reaches the value of 10. Most of the following calculations show the result of cases where Δ

is 10, but regarding the mass of the stable limit M of GMR, changes in M were calculated until Δ reaches the value of 10, and then the minimum value was used. Further, for the case of SMR, the value of M obtained when Δ is 10 was employed since M shows a flat decrease.

3. Optimal Bearing Parameters

The most prominent feature of the conical bearing is that it has both axial load capacity and radial load capacity. In this chapter, calculations for the optimal axial load capacity F_z , ingredients in the radial direction of the radial load capacity F_r , and the mass of the stable limit M will be performed with the simplex method to obtain optimized bearing parameters which can maximize F_z , F_r , and M respectively.

3.1 Optimal bearing parameters which maximize characteristics

Tables 1, 2 and 3 show parameters which can maximize F_z , F_r , and M respectively for a case where the conical angle is $\phi = 45^\circ$, the bearing constant is $\Delta = 10$, and the ratio of the total bearing area to the reference area is $A/A_0 = 1$.

Table 1 shows the optimized bearing parameters which maximize F_z . Since, in terms of the analytical principle, the characteristics in the axial direction make no difference between GMR and SMR, the optimized parameters for F_z become the same for both GMR and SMR. From the tables, we can see that SMR has a little larger F_r , but SMR a smaller M . In addition, parameters β , α and Δ of the regular and reversible-rotation type bearing has a slightly larger values comparing to those of the conventional one directional rotation type. Regarding η , we can see for the one directional rotation type of bearing that F_z becomes larger when the smooth region of $\eta = 0$ does not exist, while for the regular and reversible rotation type, we can also see that 20% of the total bearing area must be set in the smooth region. Further, we can see that F_z decreases down to 50% in the case of the regular and reversible bearing compared to the one directional rotation type of bearing.

Table 2 shows the optimized bearing parameters which maximize F_r . We can see that the optimal parameters (β , α , Δ , ν_r , η) for GMR and SMR are almost equivalent. We can also see that F_z becomes small only in the case of reversible rotation of GMR, that the other

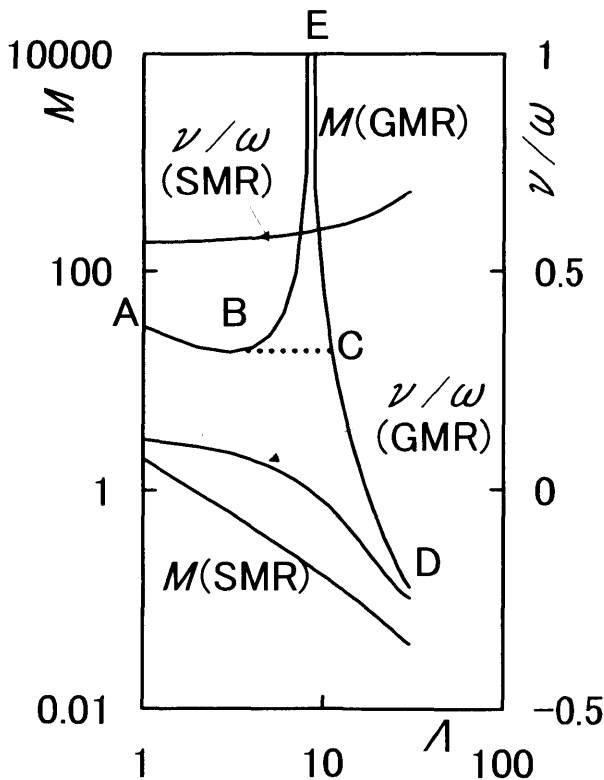


Fig4 Changes of M with Δ

parameters become almost equivalent for GMR and SMR, that F_z becomes a slightly larger for SMR, and that M becomes significantly large for GMR. We can see that optimized parameters of the regular and reversible-rotation type of bearing have a slightly larger values on β , α , Δ and η when compared to those of the conventional one directional rotation type. It is known that in the case of the regular and reversible-rotation type of bearing, F_r becomes around 55% of the conventional one directional rotation type.

The optimized bearing parameters which maximize M shown in Table 3, show that GMR has larger optimized parameters for α and Δ , smaller values for β and γ_r ,

and that η becomes equivalent for GMR and SMR. We can see that SMR has significantly larger F_z and F_r , and GMR has a significantly larger M . Regarding the optimized parameters for the regular and reversible-rotation type of bearing, it is known that compared to the case of the conventional one directional rotation type, GMR has larger β and η , and SMR has smaller α , Δ and η . In addition, we can see that in the case of the regular and reversible-rotation type of bearing, M becomes about 70% and 35% of the one directional rotation type for GMR and SMR respectively. It follows from what has been said, that in the case of the

Table 1 Optimized bearing parameters for F_z ($\Delta=10$, $\phi=45^\circ$, $A/A_0=1$)

		β°	α	Δ	γ_r or γ_c	η	F_z		F_r		M	
							$+\omega$	$-\omega$	$+\omega$	$-\omega$	$+\omega$	$-\omega$
Present Type	GMR								0.086	0.231	12.6	0.616
	SMR	17.9	0.64	3.11	0.41	0.20	0.178	0.178	0.140	0.289	0.029	0.046
Conventional Type	GMR								0.307		2.96	
	SMR	15.7	0.50	2.65	0.56	0	0.363		0.313		0.170	

Table 2 Optimized bearing parameters for F_r ($\Delta=10$, $\phi=45^\circ$, $A/A_0=1$)

		β°	α	Δ	γ_r or γ_c	η	F_z		F_r		M	
							$+\omega$	$-\omega$	$+\omega$	$-\omega$	$+\omega$	$-\omega$
Present Type	GMR	21.9	0.55	1.96	0.51	0.20	0.224	0.138	0.195	0.227	1.45	1.59
	SMR	19.1	0.59	2.24	0.51	0.22	0.216	0.216	0.211	0.263	0.075	0.102
Conventional Type	GMR	16.6	0.44	1.80	0.58	0.12	0.325		0.362		0.680	
	SMR	16.5	0.44	1.81	0.58	0.09	0.328		0.363		0.367	

Table 3 Optimized bearing parameters for M ($\Delta=10$, $\phi=45^\circ$, $A/A_0=1$)

		β°	α	Δ	γ_r or γ_c	η	F_z		F_r		M	
							$+\omega$	$-\omega$	$+\omega$	$-\omega$	$+\omega$	$-\omega$
Present Type	GMR	11.8	0.61	3.08	0.43	0.24	0.017	0.016	0.012	0.021	63.5	33.0
	SMR	30.1	0.37	1.32	0.51	0.24	0.172	0.101	0.215	0.201	0.167	0.334
Conventional Type	GMR	9.4	0.65	4.63	0.18	0	0.134		0.078		90.1	
	SMR	16.4	0.43	1.81	0.64	0.33	0.294		0.359		0.448	

regular and reversible-rotation type of bearing, as compared to the conventional one direction rotation type of gas-lubricated grooved bearing, the limit of F_z is down to 50%, that of F_r is to 55%, and that of M is to 70% for GMR and 35% for SMR, whatever adjustments are made on the bearing parameters.

3.2 Changes of Optimized Bearing Parameters by A and A/A_0

Figures 5 and 6 show influences (a) by A and influences (b) by A/A_0 on respective bearing parameters that maximize F_z and F_r for the case of GMR.

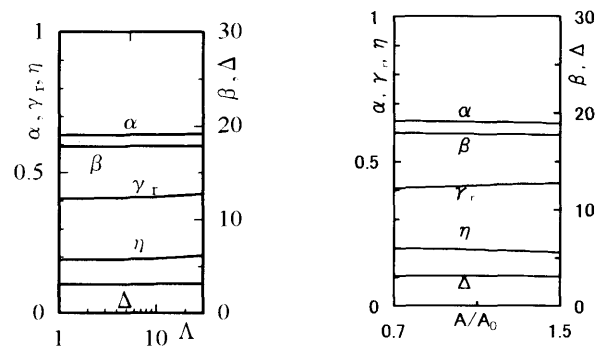
In Fig. 5, we can see that bearing parameters that maximize F_z are hardly influenced by A and A/A_0 . This tendency was also seen for SMR. We also investigated influences on various parameters that maximize M , and found that the influences were also small.

In Fig. 6, we can see that, regarding respective parameters which maximize F_r , if A takes the value of 10 or more, β will become larger, and if A takes the value of 20 or more, α shows a sharp increase, but if A is 10 or less, the respective optimal parameters will not be influenced very much. Further, regarding influences by A/A_0 , it is also known that β becomes larger as A/A_0 becomes larger, but other optimal parameters will be less influenced. Accordingly, in the following section, we will refer to the case of $A = 10$ and $A/A_0 = 1$ which are regions frequently employed for practical use and less influenced by A and A/A_0 .

4 Parameters for Bearing Profile Simultaneously Enhancing F_z and F_r

In this chapter, we will consider bearing parameters which enhance characteristics of both F_z and F_r simultaneously. To determine such optimal bearing parameters, we adopted the following procedures. First, investigations were made on influences on bearing characteristics F_z , F_r and M near optimal parameters by parameters of respective bearing types, referring to Tables 1 and 2, and presuming bearing parameters ($\beta = 20^\circ$, $\alpha = 0.6$, $\Delta = 2.4$, $\gamma_r = 0.45$, $\eta = 0.2$) which enhance characteristics of both F_z and F_r , and then by producing diagrams similar to Figures 7 through to 11 based on the presumed parameters. Based on the results obtained, the respective optimal parameters were modified, and diagrams corresponding to Figures 7 – 11

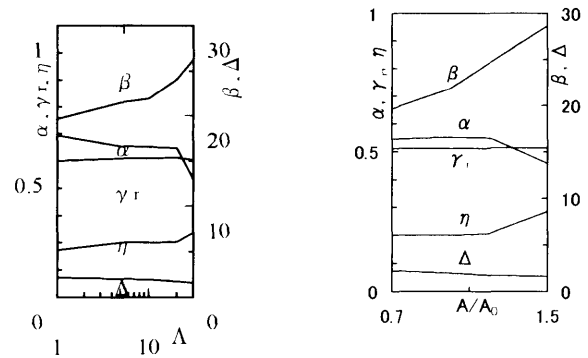
were produced again. The procedure to modify parameters was repeated several times, and then the final optimal bearing parameters were determined. Table 4 shows the optimum bearing parameters obtained through the above-stated procedure. It should be noted that Table 4 also shows, besides the optimal values, the optimal ranges (parameters that have bearing characteristics similar to the optimal values) which were obtained through evaluations of Figures 7 – 11. Figures 7 – 11 show influences by the respective parameters on the bearing characteristics F_z , F_r and M based on the optimal bearing parameters listed in Table 4, wherein values except those on the horizontal axis are with fixed values



(a) Influences of A

(b) Influences of A/A_0

Fig.5 The change of optimal bearing parameters for F_z with A and A/A_0 (GMR)



(a) Influences of A

(b) Influences of A/A_0

Fig.6 The change of optimal bearing parameters for F_r with A and A/A_0 (GMR)

Table4 Optimal bearing parameters for both of F_z/F_r of the present regular and reversible bearing (GMR and SMR, $A = 10$, $\phi = 45^\circ$, $A/A_0 = 1$)

β°	α	Δ	γ_r	η
22.5	0.5	2.0	0.55	0.2
(20 - 25)	(0.4 - 0.5)	(1.8 - 2.2)	(0.5 - 0.6)	(0.18 - 0.22)

of the optimal parameters, and the mark \triangle indicates the value of the optimal parameter. In addition, the symbol (+) indicates the regular rotation, (-) indicates the reversible rotation, G stands for GMR, and S stands for SMR in the figures. It should be noted that F_z is not classified into G and S since it is the same for both GMR and SMR. Further, the range of characteristics and optimal parameters that are to be evaluated for the regular and reversible rotation-type bearing are shown in bold lines in the figure.

4.1 Influence of β

Fig. 7 shows how the bearing characteristics change depending on β . The figure shows that:

As one of the characteristics of the regular and reversible rotation-type bearing, evaluations must be made by using characteristics for regular rotations and reverse rotations, whichever lower. Regarding F_z , however, $F_z(-)$ for the reversible rotation usually indicates lower values than $F_z(+)$ for the regular rotation. The value determined as the optimal parameter is $\beta = 22.5^\circ$, but it will almost make no difference if the value is in the range of 20° and 25° . In addition, if β becomes larger within its optimal range, F_z will be slightly larger, and F_r will also be slightly smaller. Accordingly, if greater importance is given to F_z , it would be better to set β near 25° , and if the focus is on F_r , β should be set near 20° . We can see that, in the optimal range, $F_z(-)$ will be about 50% of $F_z(+)$. Regarding F_r , the characteristics for reversible rotation become larger in the optimal range for both GMR and SMR. The same applies to the subsequent figures 8 through 11. The parameter M shows an almost constant value around the optimal value, and GMR presents higher stability than SMR. This tendency also applies to other parameters.

4.2 Influence of α

Fig. 8 shows how the bearing characteristics depend on α . The figure shows that:

The value determined as the optimal parameter is $\alpha = 0.5$, but there will be almost no difference if the value is in the range of 0.4 and 0.6. In addition, if α becomes larger within its optimal range, F_z will be slightly larger, and F_r will be slightly smaller. Accordingly, if greater importance is given to F_z , it would be better to set α near 0.6, and if the focus is on F_r , α should be set near 0.4.

4.3 Influence of Δ

Fig. 9 shows how the bearing characteristics depend on Δ . The figure shows that:

The value determined as the optimal parameter is $\Delta = 2.0$, but there will be almost no difference if the value is between 1.8 and 2.2. In addition, if Δ becomes larger within its optimal range, F_z will be slightly larger, and F_r will be slightly smaller. Accordingly, if greater importance is given to F_z , it would be better to set Δ near 2.2, and if the focus is on F_r , Δ should be set near 1.8.

4.4 Influence of γ_r

Fig. 10 shows how the bearing characteristics influenced by γ_r . The figure shows that:

The value determined as the optimal parameter is $\gamma_r = 0.55$, but there will be almost no difference if the value is between 0.5 and 0.6.

4.5 Influence of η

Fig. 11 shows how the bearing characteristics depend on η . The figure shows that:

The value determined as the optimal parameter is $\eta = 0.2$ but there will be almost no difference if the value is between 0.18 and 0.22. In addition, if η becomes larger within its optimal range, F_z will be slightly larger, and F_r will be slightly smaller. Accordingly, even in case the value is within the range of 0.18 and 0.22, if greater importance is given to F_z , it would be better to set η near 0.22, and if the focus is on F_r , η should be set near 0.18.

5. Conclusion

From what has been said above, we can conclude that:

1. We have verified that both axial characteristics and radial characteristics can be simultaneously generated, by expanding our ideas and devices which enable the understanding of regular and reversible rotations of hydro-dynamic grooved bearings proposed by the authors also to the conical grooved bearings.
2. We have obtained optimal bearing parameters which independently optimize the bearing characteristics (load capacity in axial direction, load capacity in radial direction, and mass of the stable limit).
3. We have found the optimal bearing parameters which enhance the load capacity in the axial and

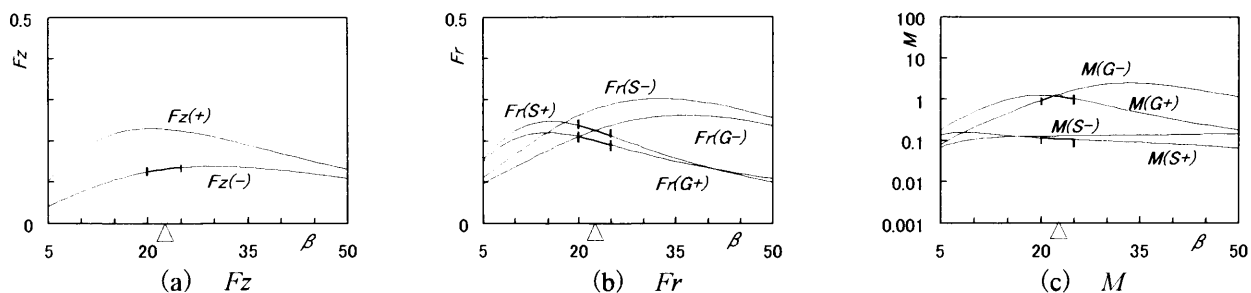


Fig.7 Changes of bearing characteristics with β near the optimal parameters ($\Lambda=10$, $\phi=45^\circ$, $A/A_0=1$)

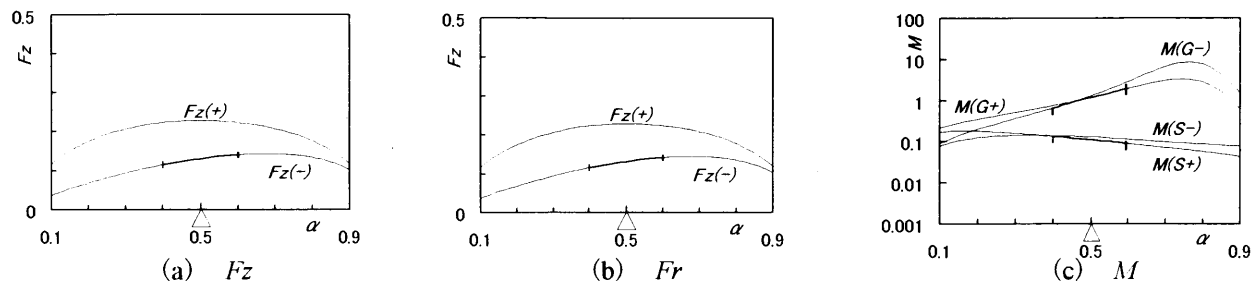


Fig.8 Changes of bearing characteristics with α near the optimal parameters ($\Lambda=10$, $\phi=45^\circ$, $A/A_0=1$)

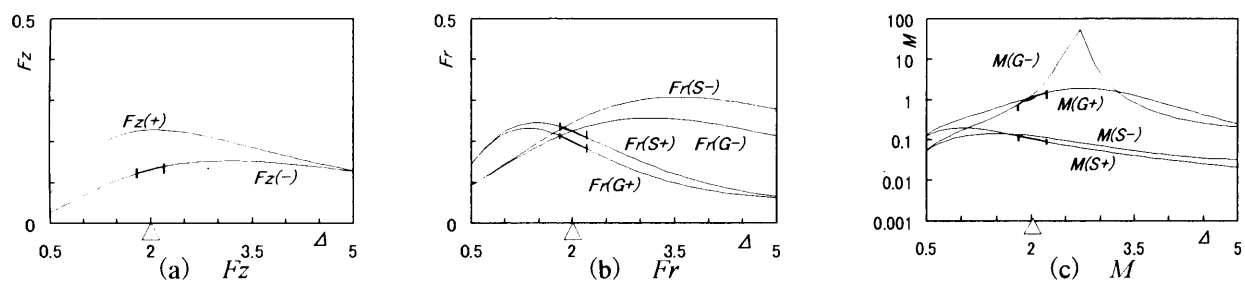


Fig.9 Changes of bearing characteristics with Δ near the optimal parameters ($\Lambda=10$, $\phi=45^\circ$, $A/A_0=1$)

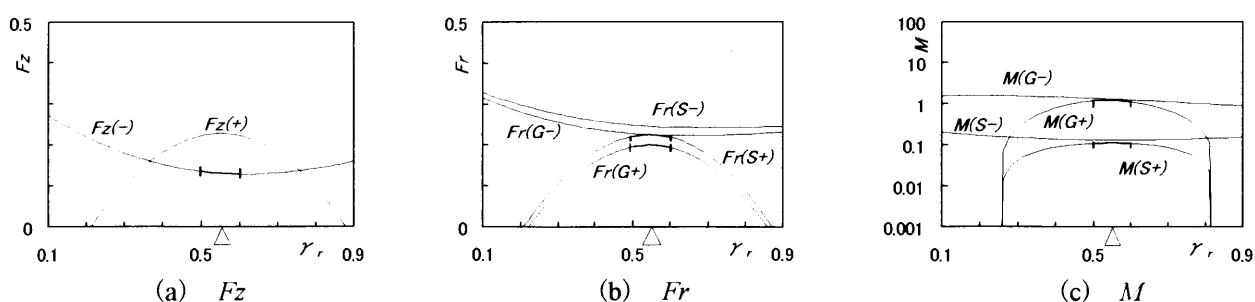


Fig.10 Changes of bearing characteristics with γ_r near the optimal parameters ($\Lambda=10$, $\phi=45^\circ$, $A/A_0=1$)

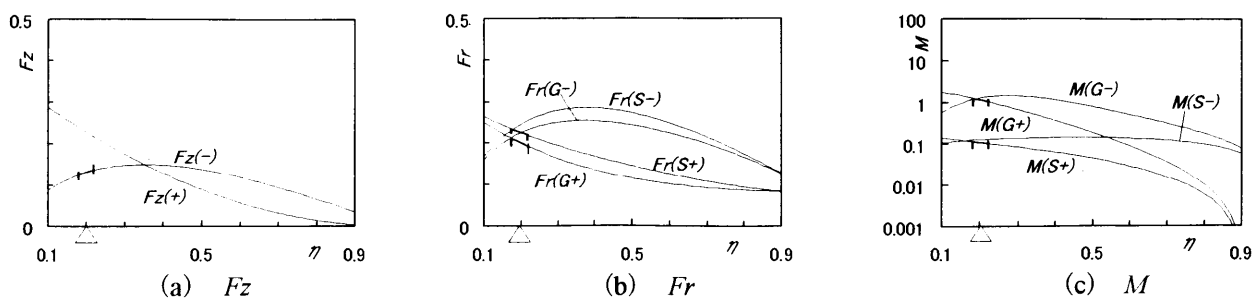


Fig.11 Changes of bearing characteristics with η near the optimal parameters ($\Lambda=10$, $\phi=45^\circ$, $A/A_0=1$)

radial direction simultaneously, and obtained results as shown in Table 4.

References

- [1] Muijderman, E.A.: Spiral Groove Bearing, Phillips Technical Library, 116 (1966).
- [2] Bootsma, J.: Liquid Lubricated Spiral-Groove Bearings, 129 (1975).
- [3] Fukuyama/Someya: Trans. Jpn. Mech. Eng., 46-410, C, 1285 (1980).
- [4] Kawabata/Ozawa/Miyake: Trans. Jpn. Mech. Eng., 58-555, C, 3355 (1992).
- [5] Kawabata/Ozawa/Miyake/Shimada: Trans. Jpn. Mech. Eng., 59-568, C, 3928 (1993).
- [6] Hsing, F.C.: Trans. ASME, Ser.F, 94-1, 81 (1972).
- [7] Kawabata/Ashino/Sekizawa/Yamazaki: Trans. Jpn. Mech. Eng., 56-528, C, 2194 (1990).

